frontiers in Marine Science

ORIGINAL RESEARCH
published: 05 October 2020
doi: 10.3389/fmars.2020.544037

Postmortem Neuroimaging of Cetacean Brains Using Computed Tomography and Magnetic Resonance Imaging

Brian C. W. Kot[1,2], Henry C. L. Tsui[1], Tabris Y. T. Chung[1] and Amy P. Y. Lau[3]*

[1] State Key Laboratory of Marine Pollution, City University of Hong Kong, Hong Kong, China, [2] Department of Veterinary Clinical Sciences, Jockey Club College of Veterinary Medicine and Life Sciences, City University of Hong Kong, Hong Kong, China, [3] School of Medical and Health Sciences, Tung Wah College, Hong Kong, China

Postmortem computed tomography (PMCT) and postmortem magnetic resonance (PMMR) imaging (PMMRI) have been applied to provide vital or additional information for conventional necropsy, along the pioneering virtopsy-driven cetacean stranding response program in Hong Kong waters. It is common for stranded carcasses to become badly degraded and susceptible to rapid cerebral autolysis and putrefaction. Necropsy on decomposed brains with limited sample analysis often defy a specific diagnosis. Studies on PMMR neuroimaging have focused on neuroanatomy and brain morphology in freshly deceased or preserved specimens. Moreover, the literature is devoid of any reference on the potential value of PMMRI examination of decomposed cetacean brains. To that end, this project evaluated the benefits of PMMR neuroimaging *in situ* in decomposed carcasses in comparison to PMCT. A total of 18 cetacean carcasses were studied by PMCT and PMMRI examinations. Anatomical brain structures and visible brain pathologies were evaluated and scored using Likert-scale rating. Intracranial gas accumulation was clearly depicted in all cases by all radiological techniques. Other features were more clearly depictable in PMMRI than in PMCT images. Results of this study indicated that superiority of PMMRI compared to PMCT increased with advanced putrefaction of the brain. The preservation of structural integrity was presented by PMMRI due to its superior capability to evaluate soft tissue. Brain PMMRI should be incorporated in postmortem investigation of decomposed stranded cetaceans.

Keywords: postmortem, magnetic resonance imaging, computed tomography, cetacean, decomposed brain

OPEN ACCESS

Edited by:
Debra Lee Miller,
The University of Tennessee, Knoxville, United States

Reviewed by:
Dominic Gascho,
University of Zurich, Switzerland
Garyfalia Ampanozi,
University of Zurich, Switzerland

****Correspondence:***
Brian C. W. Kot
briankot@yahoo.co.uk

Specialty section:
This article was submitted to Marine Megafauna, a section of the journal Frontiers in Marine Science

Received: *19 March 2020*
Accepted: *25 August 2020*
Published: *05 October 2020*

Citation:
Kot BCW, Tsui HCL, Chung TYT and Lau APY (2020) Postmortem Neuroimaging of Cetacean Brains Using Computed Tomography and Magnetic Resonance Imaging. Front. Mar. Sci. 7:544037. doi: 10.3389/fmars.2020.544037

INTRODUCTION

Virtopsy using postmortem computed tomography (PMCT) and postmortem magnetic resonance (PMMR) imaging (PMMRI) has been implemented in the pioneering virtopsy-driven cetacean stranding response program in Hong Kong (HK) waters, to provide vital or additional information for conventional necropsy (Kot et al., 2016, 2018, 2019, 2020; Chan et al., 2017; Yuen et al., 2017). Stranded cetacean carcasses found in HK waters are often badly degraded (Jefferson et al., 2002) as high temperature and humidity accelerate

autolysis (Klein et al., 2016), hampering stranding response personnel and veterinarians in the documentation of postmortem findings and tissue sampling (Tsui et al., 2020).

For decades, mammalogists and comparative neuroanatomists have been interested in cetacean brains because they are highly divergent from other mammals. Neuropathology induced by *Brucella ceti* and cetacean morbillivirus infection in stranded cetaceans were reported worldwide (Hernández-Mora et al., 2008; Raga et al., 2008), affecting the central nervous system, resulting in fatal acute or chronic meningoencephalitis. Documentation of brain morphology could be useful not only to study pathology, comparative anatomy and development of cetacean brains, but also to investigate emerging threats to stranded cetaceans such as anthropogenic chemicals (Houde et al., 2006; McKinney et al., 2006) and biotoxins from algal blooms (Broadwater et al., 2018).

Cerebral autolysis is one of the earliest postmortem changes, which could occur even in a human corpse with well-preserved condition (Levy et al., 2010). The susceptibility of brain to rapid autolysis and putrefaction is due to its high water content, leading to discolouration, softening and liquefaction at an early stage of decomposition (Klein et al., 2016). In conventional autopsy, the dissection of the cranial cavity to explore the brain and other cranial structures is complex and time-consuming, and in the case of a decomposed brain, it often defies a specific diagnosis (Klein et al., 2016). Limited valuable sample analysis could be undertaken in decomposed brains, hindering a full differential diagnosis.

Postmortem neuroimaging techniques offer a precise observation of the internal structures of the nervous system, especially in a softened or liquefied brain, when sectioning and other examinations are not practical (Thali et al., 2003b; Pfefferbaum et al., 2004; Smith et al., 2012). The brain is kept completely intact during postmortem imaging, therefore spatial distortion associated with histological processing could be minimised. The ability to pay less concern on radiation exposure and lack of motion artefacts permitted high resolution of postmortem neuroimaging (Christe et al., 2010; Gascho et al., 2018). In humans, PMCT on postmortem neuroimaging is mostly used to examine foreign bodies, skull fractures, and gas accumulation inside the brain (Levy et al., 2010). PMMRI is complementary to PMCT, which specialises in depicting brain lesions and parenchymal pathologies (Flach et al., 2016).

Evaluation of postmortem changes in adipose tissues of dolphin heads has been performed using PMCT and PMMRI (Mckenna et al., 2007; Arribart et al., 2018), suggesting that these postmortem analyses are associated with each other and add value to represent their living biological counterpart. Studies on *in situ* PMMR neuroimaging have mainly focused on the neuroanatomy and brain morphology of isolated cases of freshly deceased cetaceans (Montie et al., 2007) or preserved specimens (Oelschläger et al., 2010). Limited access to PMMRI units, time

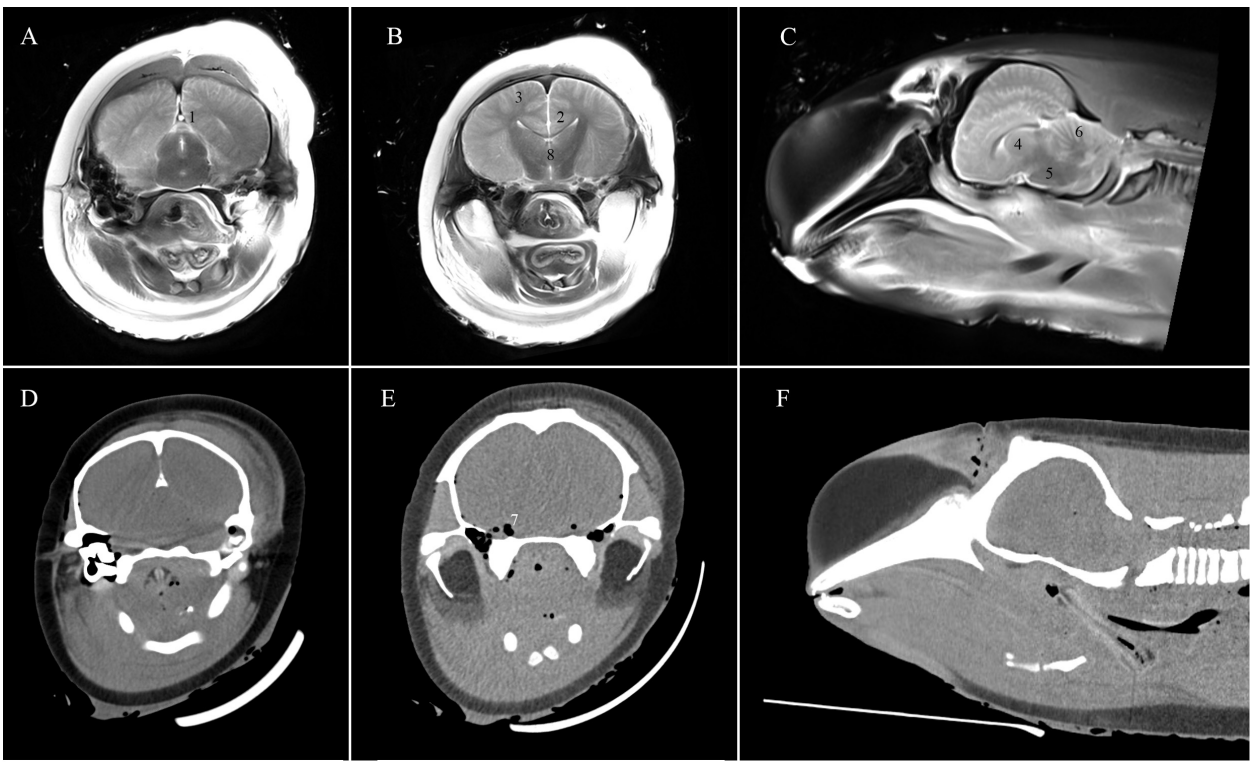

FIGURE 1 | T2w PMMR **(A–C)** and PMCT **(D–F)** images illustrating the eight regions of interest of the cetacean brain for the evaluation: (1) dorsal sagittal sinus; (2) ventricles; (3) grey and white matter junction; (4) basal ganglia; (5) brain stem; (6) cerebellum; (7) intracranial gas accumulation; (8) brain midline/symmetry.

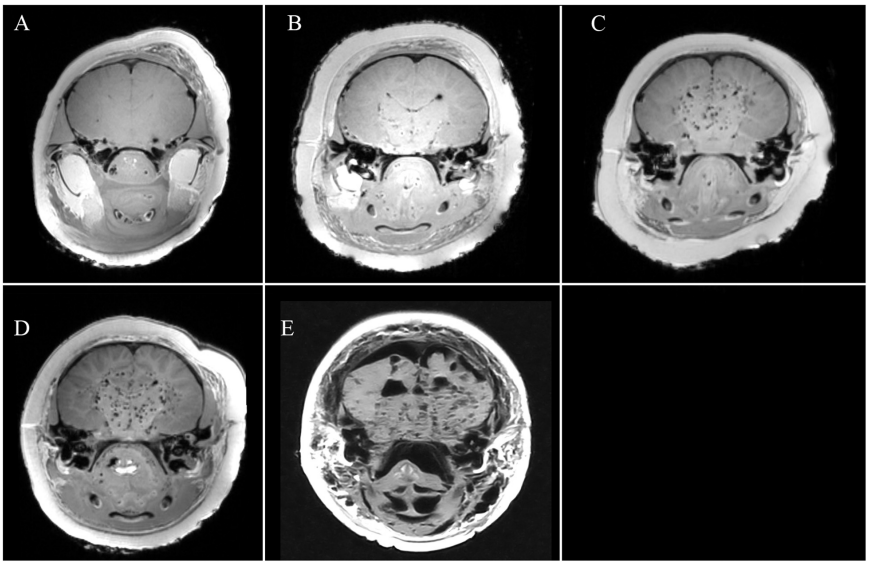

FIGURE 2 | T1w PMMRI of the cetacean brain demonstrating five criteria of analysis: **(A)** clearly depicted; **(B)** indicated; **(C)** partly indicated; **(D)** barely identifiable; **(E)** not identifiable.

constraints and the complexity of PMMRI technical principles and parameters are thought to be the main reasons why PMMRI is used less frequently than PMCT. To the best of our knowledge, formal literature is devoid of any reference on the potential values of PMMRI examination of decomposed cetacean brains. This present study aimed to evaluate and describe the possible benefits of PMMR neuroimaging *in situ* in decomposed cetacean carcasses in comparison to PMCT.

MATERIALS AND METHODS

Subjects

A total of 18 carcasses (9 males and 9 females, including calf to adult; 77–235 cm in length) of 2 cetacean species, i.e., Indo-Pacific finless porpoise (*Neophocaena phocaenoides*) and Indo-Pacific humpback dolphin (*Sousa chinensis*), stranded in 2014–2019, were included in the study. The conditions of the carcasses ranged from code 2 to code 3 (Geraci and Lounsbury, 2005).

Postmortem Neuroimaging Protocols

The carcasses were contained in artefact-free body bags for PMCT and PMMRI scanning. All subjects were examined in a prone position for PMCT, immediately followed by PMMRI in the same timeslot.

PMCT Image Acquisition

All PMCT brain examinations were conducted with a Siemens 64-row multi-slice spiral CT scanner Somatom go.Up (Siemens Healthineers, Germary). The scans were operated at 80 to 130 kV, 60 to 200 mA, and 1 mm slice thickness. Scan field of view (sFOV) ranged from 15.8 to 53.4 cm.

PMMR Image Acquisition

All PMMRI brain examinations were conducted with a GE SIGNA Explorer 1.5 Tesla MR scanner with a standard quadrature head coil (General Electric Company, Wisconsin, United States). The following MR sequences were applied: T1-weighted (T1w) transverse, T1w coronal, T1w sagittal (192 slices, 1 mm thickness, TR 1900 ms, TE 2.5 ms; T2-weighted (T2w) transverse, T2w coronal, T2w sagittal (192 slices, 1 mm thickness, TR 5000 ms, TE 93 ms). Reconstructed matrix of 640 × 640 and FOV of 320 × 280 mm were used.

Image Processing and Evaluation

Volumetric data was reconstructed and reformed for multiplanar reconstruction using TeraRecon Aquarius iNtuition workstation (TeraRecon Inc., San Mateo, CA). The rendered PMCT and PMMR images were viewed with brain window settings (PMCT: window width, 350 HU; window level, 70 HU; PMMRI: window width, 1000; window level, 500). Image evaluation was performed by a diagnostic radiographer and imaging researcher (BK) certified by local and international human boards, who had more than 6 years of experience in postmortem imaging and cetacean virtopsy interpretation.

Criteria of Analysis

Anatomical brain structures (dorsal sagittal sinus, ventricles, grey and white matter junction, basal ganglia, brain stem, and cerebellum), and visible brain pathologies (intracranial gas accumulation, and brain midline/symmetry) were evaluated by PMCT, T1w PMMRI, and T2w PMMRI (**Figure 1**) and scored using Likert-scale rating with reference to the following criteria:

> Clearly depicted, 4 points – the intracranial anatomy around the organ of interest and any brain pathology could

be accurately recognised and diagnosed (**Figure 2A**);

Indicated, 3 points – the anatomical structures were slightly altered due to postmortem changes but brain pathology could still be recognised with a level of certainty (**Figure 2B**);

Partly indicated, 2 points – the anatomical structures could be identified but were severely decomposed and no pathology could be diagnosed due to the alteration (**Figure 2C**);

Barely identifiable, 1 point – allowance of basic recognition of the anatomical structures but too autolysed for pathological diagnosis (**Figure 2D**);

Not identifiable, 0 point – the anatomical structure could not be recognised in the image (**Figure 2E**).

The evaluation scores for each anatomical structure or pathology were summed and converted to evaluation rates for each radiological techniques. The maximum score in which all cases were clearly depicted was 4 points × 18 cases = 72 points (100% evaluation rate). First quartile, median, and third quartile of evaluation scores for each feature were also calculated for each radiological technique.

Experimental procedures in this study were reviewed and approved by the Agriculture, Fisheries and Conservation Department of Hong Kong Special Administrative Region [AF GR CON 09/68 PT.15]. All examinations were undergone in accordance with relevant guidelines and regulations.

RESULTS

Results of the image evaluation are reported in **Table 1**. Intracranial gas accumulation was clearly depicted in all cases by all radiological techniques. Brain midline/symmetry was clearly depicted in 17 out of 18 cases by PMMRI but not identifiable in all cases by PMCT. For the six anatomical features, evaluation scores of T2w PMMRI were higher than that of T1w PMMRI. For PMCT, ventricles were at least identifiable in 10 cases and the cerebellum was partly indicated in 2 cases. Dorsal sagittal sinus, grey and white matter junction, basal ganglia, brain stem and brain midline/symmetry were not identifiable by PMCT.

Summary of the evaluation is shown in **Table 2**. All radiological techniques achieved 100% evaluation rate for intracranial gas accumulation. Evaluation rate of brain midline/symmetry was 96% for both T1w and T2w PMMRI, and 0% for PMCT. For the 6 regions of interest, evaluation rate ranged from 71 to 83% for T1w PMMRI, 90 to 100% for T2w PMMRI, and 0 to 26% for PMCT. PMMR images were assigned higher evaluation scores (medians: 3.5–4) compared to PMCT (medians: 0–1, except for intracranial gas accumulation), indicating that the features were better depicted in PMMRI than in PMCT images.

TABLE 1 | Evaluation scores of the eight regions of interest of the cetacean brain with reference to the criteria of analysis in PMCT, T1w PMMRI, and T2w PMMRI using Likert-scale rating.

Evaluation score in Likert-scale

Region of interest	PMCT																	
Dorsal sagittal sinus	0	0	0	0	0	0	0	0	0	0	0	0	0	0	0	0	0	0
Ventricles	0	4	0	0	0	0	2	2	0	2	1	0	1	1	1	1	0	4
Grey and white matter junction	0	0	0	0	0	0	0	0	0	0	0	0	0	0	0	0	0	0
Basal ganglia	0	0	0	0	0	0	0	0	0	0	0	0	0	0	0	0	0	0
Brain stem	0	0	0	0	0	0	0	0	0	0	0	0	0	0	0	0	0	0
Cerebellum	0	2	0	0	0	0	0	0	0	0	0	0	0	0	0	0	0	2
Intracranial gas accumulation	4	4	4	4	4	4	4	4	4	4	4	4	4	4	4	4	4	4
Brain midline/symmetry	0	0	0	0	0	0	0	0	0	0	0	0	0	0	0	0	0	0

Region of interest	PMMRI (T1w)																	
Dorsal sagittal sinus	4	4	4	4	4	4	4	2	4	2	2	2	2	2	2	4	1	4
Ventricles	4	4	4	4	4	4	4	4	4	1	3	3	2	1	3	1	2	4
Grey and white matter junction	4	4	3	4	4	4	4	4	4	1	3	2	1	1	4	3	0	4
Basal ganglia	4	4	4	4	4	4	4	1	4	2	2	2	1	1	3	2	1	4
Brain stem	4	4	4	4	4	4	4	1	4	2	1	3	2	2	2	2	0	4
Cerebellum	4	4	4	4	4	4	4	4	4	2	3	3	2	2	4	3	1	4
Intracranial gas accumulation	4	4	4	4	4	4	4	4	4	4	4	4	4	4	4	4	4	4
Brain midline/symmetry	4	4	4	4	4	4	4	4	4	4	4	4	4	4	4	4	1	4

Region of interest	PMMRI (T2w)																	
Dorsal sagittal sinus	4	4	4	4	4	4	4	2	4	2	4	4	4	4	4	4	1	4
Ventricles	4	4	4	4	4	4	4	4	4	4	4	4	4	4	4	4	4	4
Grey and white matter junction	4	4	3	4	4	4	4	4	4	4	4	4	4	4	4	4	2	4
Basal ganglia	4	4	4	4	4	4	4	4	4	4	4	4	4	4	4	4	1	4
Brain stem	4	4	4	4	4	4	4	4	4	4	4	4	4	4	4	4	0	4
Cerebellum	4	4	4	4	4	4	4	4	4	4	4	4	4	4	4	4	2	4
Intracranial gas accumulation	4	4	4	4	4	4	4	4	4	4	4	4	4	4	4	4	4	4
Brain midline/symmetry	4	4	4	4	4	4	4	4	4	4	4	4	4	4	4	4	1	4

4 = Clearly depicted. 3 = Indicated. 2 = Partly indicated. 1 = Barely identifiable. 0 = Not identifiable.

TABLE 2 | Radiological assessment on the eight regions of interest of the cetacean brain using Likert-scale rating.

Region of interest	Evaluation rate (%)			Median of evaluation scores (Q1–Q3)		
	PMCT	PMMRI (T1w)	PMMRI (T2w)	PMCT	PMMRI (T1w)	PMMRI (T2w)
Dorsal sagittal sinus	0	76	90	0 (0–0)	4 (2–4)	4 (4–4)
Ventricles	26	78	100	1 (0–1.75)	4 (2.25–4)	4 (4–4)
Grey and white matter junction	0	75	96	0 (0–0)	4 (2.25–4)	4 (4–4)
Basal ganglia	0	71	96	0 (0–0)	3.5 (2–4)	4 (4–4)
Brain stem	0	71	94	0 (0–0)	3.5 (2–4)	4 (4–4)
Cerebellum	6	83	97	0 (0–0)	4 (3–4)	4 (4–4)
Intracranial gas accumulation	100	100	100	4 (4–4)	4 (4–4)	4 (4–4)
Brain midline/symmetry	0	96	96	0 (0–0)	4 (4–4)	4 (4–4)

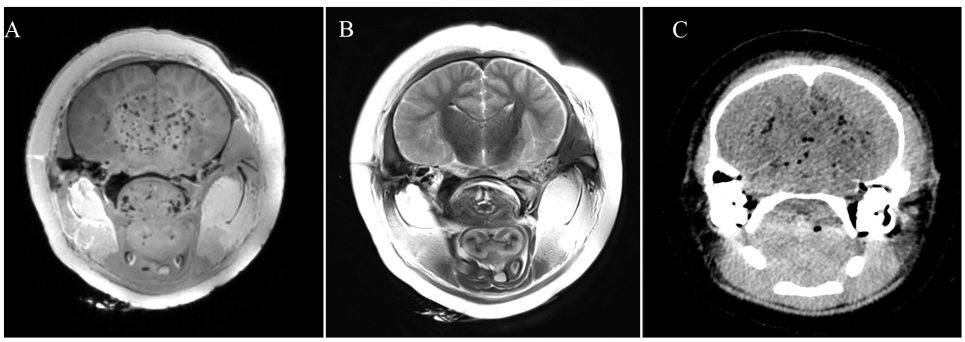

FIGURE 3 | Intracranial gas accumulation affected image quality in **(A)** T1w PMMRI; **(B)** T2w PMMRI; and **(C)** PMCT.

There were no abnormal focal areas of altered attenuation or signal intensity in the cerebral hemispheres, brainstem or cerebellum in all PMCT and PMMRI examinations. Appearance, attenuation, and intensity of brain parenchyma were unremarkable. The ventricular system appeared unremarkable. No evidence of intracranial space occupying lesion or obvious vascular anomaly was noted.

DISCUSSION

Unlike clinical MRI examinations with contrast enhanced sequences and organ perfusion, PMMRI relied on the sole morphological presentation of the investigated structures since only structural tissue alterations alter image contrast (Jackowski et al., 2010). In human forensic medicine, PMMRI is a modality that is mostly complementary to PMCT in detecting soft tissue lesions and parenchymal pathologies, with the fact that PMMRI alone is more prone to artefacts from gas and foreign bodies. Recent modification of a three-dimensional fast-field-echo sequence with multiple echoes for specific bone imaging on PMMRI might also allow visualisation of beveled fractures as well as radiating bone fracture lines, which is equivalent to PMCT regarding the visualisation of bone damage in craniocerebral gunshot injuries (Gascho et al., 2020). In addition, it was suggested that adequate professional radiological training is essential for performing and reporting PMMRI (Cartocci et al., 2020). The heavy expenditures of machine acquisition and maintenance and the time-consuming operation of PMMRI also lead to its less frequent usage than PMCT. Time-related course of image findings in PMMRI of experimental animal models have been mentioned in the literature (Calabrese et al., 2015; Henes et al., 2017). However, those studies mainly conducted with small numbers of isolated cases. Thus far, no detailed study elaborating the potential advantage of PMMRI on decomposed brain in stranded cetaceans has been published. This study indicated the superior capability of PMMRI compared to PMCT in depicting soft tissue and preservation of structural integrity increased with advancing putrefaction in the brain.

In the present study, the postmortem brain generally presented on PMCT with a blurring of the sulci effacement and loss of the corticomedullary differentiation. This observation greatly aggravates the detection of agonal or antemortem brain oedema (Flach et al., 2016). On PMMRI, this effect is less visible. Despite the presence of the aforesaid postmortem signal changes, grey and white matter was still clearly depicted with a distinct soft tissue contrast, allowing a better image evaluation of pathologies. This might explain why brain structures could be mostly identifiable and be clearly depicted with PMMRI in some of our subjects.

Gas is a common virtopsy finding in decomposition, but it may also arise from cases involving fatal and non-fatal gas embolism, or pathology (Gebhart et al., 2012). In this study, both PMCT and PMMRI could clearly depict intracranial gas accumulation in all cases (**Figure 3**). Postmortem gas in the vascular system can provide a negative contrast in PMCT brains

(Cartocci et al., 2020). However, gas accumulation may degrade image quality on PMMRI to a greater extent than on PMCT, since the PMMR signal intensity can be decreased, especially during the T1w sequence image acquisition, due to changes in the soft tissue chemical properties (Lundström et al., 2012). This might explain why brain structures could not be clearly depicted, and in some of our subjects, were barely identifiable with T1w PMMR images.

One limitation of the present study was that carcass temperature was not recorded, forbidding the investigation on the influence of changes in subject temperature on the PMMR image quality. Temperature is not considered to be an influencing factor on image quality of PMCT as it is on that of PMMR. On the contrary, image contrast in PMMRI is temperature-dependent, as T1 and T2 relaxation times are greatly affected by the temperature of the subject. Previous studies in humans demonstrated that different, and particularly low corpse temperatures may alter image quality in PMMRI (Thali et al., 2003a; Zech et al., 2015). In the present study, carcasses were kept out of the freezer for 24 h prior to the PMMRI examinations, and the PMMRI examination room temperatures ranged from 16 to 22°C. At these temperatures, the image quality was appeared optimal with sufficient grey value contrast. However, in cases with lower corpse temperatures, image quality and recognisability of brain structures could be significantly affected (Flach et al., 2016). Rectal temperature measurements of cetacean carcasses before and after PMMRI are suggested to facilitate a retrospective evaluation of the correlation between body temperature and PMMR image quality in both research and clinical setting in future studies.

Another limitation of the present study was the lack of variety on choices of PMMRI sequence for comparative evaluation of cetacean neuroimaging. PMMRI sequences such as fluid-attenuated inversion recovery, diffusion-weighted image and tensor image sequences were excluded due to the time constraints in image acquisition. These advanced PMMRI techniques have not yet been fully explored. Yen et al. (2006) described the potential application of diffusion tensor imaging of traumatic fibre tract rupture in human with a brain stem lesion. Scheurer et al. (2011) examined 20 human cases with diffusion-weighted and tensor imaging to estimate the postmortem interval, and suggested that the apparent diffusion coefficient could be an indicator for the assessment of the postmortem interval. Further study on the application of various PMMRI sequences for cetacean neuroimaging is suggested to investigate their potential values and implications.

To conclude, results of the present study demonstrated that PMMRI of decomposed brains offered a more distinct soft tissue contrast and allowed detailed morphological assessment of decomposed brains compared to PMCT. Brain PMMRI should be incorporated in postmortem investigation of decomposed cetacean carcasses.

DATA AVAILABILITY STATEMENT

The datasets generated for this study will not be made publicly available due to restrictions from the Agriculture, Fisheries and Conservation Department of Hong Kong Special Administrative Region. The raw data supporting the conclusions of this article can be made available by contacting Dr. Ng Wai-Chuen (waichuen_ng@afcd.gov.hk), upon reasonable request.

ETHICS STATEMENT

Ethical review and approval was not required for the animal study because research activities coincided with the Local Cetacean Stranding Response Programme in Hong Kong, sanctioned by the Agriculture, Fisheries and Conservation Department of Hong Kong Special Administrative Region.

AUTHOR CONTRIBUTIONS

BK, HT, and AL wrote the first draft of the manuscript. All authors contributed to the conception and design of the study, analysed the data, and wrote sections of the manuscript. All authors also contributed to the field work and the data collection, contributed to the manuscript revision, and read and approved the submitted version.

FUNDING

This project was funded by the Hong Kong Research Grants Council (Grant No: UGC/FDS17/M07/14), and the Marine Ecology Enhancement Fund (Grant Nos: MEEF2017014, MEEF2017014A, MEEF2019010, and MEEF2019010A), the Marine Ecology & Fisheries Enhancement Funds Trustee Limited. All the funding was awarded to BK (project leader and principal investigator of the funded projects).

ACKNOWLEDGMENTS

We would like to thank the Agriculture, Fisheries and Conservation Department of the Hong Kong Special Administrative Region Government for the continuous support in this project. Sincere appreciation is also extended to veterinarians, staff, and volunteers from the Aquatic Animal Vitropsy Lab, City University of Hong Kong, Ocean Park Conservation Foundation Hong Kong and Ocean Park Hong Kong, for paying great effort on the stranding response in this project. Special gratitude is owed to radiological technicians in CityU Veterinary Medical Centre for operating the computed tomography and magnetic resonance imaging units in the present study. Any opinions, findings, conclusions or recommendations expressed herein do not necessarily reflect the views of the Marine Ecology Enhancement Fund or the Trustee. Special thanks to Dr. María José Robles Malagamba for English editing of this manuscript.

REFERENCES

Arribart, M., Ognard, J., Tavernier, C., Richaudeau, Y., Guintard, C., Dabin, W., et al. (2018). Comparative anatomical study of sound production and reception systems in the common dolphin (*Delphinus delphis*) and the harbour porpoise (*Phocoena phocoena*) heads. *Anat. Histol. Embryol.* 47, 3–10. doi: 10.1111/ahe.12305

Broadwater, M. H., Van Dolah, F. M., and Fire, S. E. (2018). "Vulnerabilities of marine mammals to harmful algal blooms," in *The Harmful Algal Blooms: A Compendium Desk Reference*, eds S. E. Shumway, J. M. Burkholder, and S. L. Morton (Hoboken, NJ: John Wiley & Sons), 191–222. doi: 10.1002/9781118994672.ch5

Calabrese, E., Badea, A., Cofer, G., Qi, Y., and Allan Johnson, G. (2015). A diffusion MRI tractography connectome of the mouse brain and comparison with neuronal tracer data. *Cereb. Cortex.* 25, 4628–4637. doi: 10.1093/cercor/bhv121

Cartocci, G., Santurro, A., Frati, P., Guglielmi, G., La Russa, R., and Fineschi, V. (2020). "Imaging techniques for postmortem forensic radiology," in *Radiology in Forensic Medicine*, eds G. Lo Re, A. Argo, M. Midiri, and C. Cattaneo (Cham: Springer), 29–42. doi: 10.1007/978-3-319-96737-0_5

Chan, D. K. P., Tsui, H. C. L., and Kot, B. C. W. (2017). Database documentation of marine mammal stranding and mortality: current status review and future prospects. *Dis. Aquat. Org.* 126, 247–256. doi: 10.3354/dao03179

Christe, A., Flach, P., Ross, S., Spendlove, D., Bolliger, S., Vock, P., et al. (2010). Clinical radiology and postmortem imaging (Virtopsy) are not the same: specific and unspecific postmortem signs. *Leg. Med. (Tokyo)* 12, 215–222. doi: 10.1016/j.legalmed.2010.05.005

Flach, P. M., Gascho, D., Ruder, T. D., Franckenberg, S., Ross, S. G., Ebner, L., et al. (2016). "Postmortem and forensic magnetic resonance imaging," in *Imaging of the Pelvis, Musculoskeletal System, and Special Applications to CAD*, Vol. 19, ed. L. Saba (Boca Raton, FL: CRC Press), 455–482. doi: 10.1201/b19531-20

Gascho, D., Thali, M. J., and Niemann, T. (2018). Post-mortem computed tomography: technical principles and recommended parameter settings for high-resolution imaging. *Med. Sci. Law* 58, 70–82. doi: 10.1177/0025802417747167

Gascho, D., Zoelch, N., Tappero, C., Kottner, S., Bruellmann, E., Thali, M. J., et al. (2020). FRACTURE MRI: optimized 3D multi-echo in-phase sequence for bone damage assessment in craniocerebral gunshot injuries. *Diagn. Interv. Imaging* 101, 611–615. doi: 10.1016/j.diii.2020.02.010

Gebhart, F. T. F., Brogdon, B. G., Zech, W., Thali, M. J., and Germerott, T. (2012). Gas at postmortem computed tomography – an evaluation of 73 non-putrefied trauma and non-trauma cases. *Forensic. Sci. Int.* 222, 162–169. doi: 10.1016/j.forsciint.2012.05.020

Geraci, J. R., and Lounsbury, V. J. (2005). *Marine Mammals Ashore: A Field Guide for Strandings*. Baltimore: National Aquarium in Baltimore.

Henes, F. O., Regier, M., Bannas, P., Henker, M., Heinemann, A., Sperhake, J., et al. (2017). Early time-related course of image findings in postmortem MRI: typical findings and observer agreement in a porcine model. *Leg. Med. (Tokyo)* 28, 15–21. doi: 10.1016/j.legalmed.2017.07.005

Hernández-Mora, G., González-Barrientos, R., Morales, J., Chaves-Olarte, E., Guzmán-Verri, C., Baquero-Calvo, E., et al. (2008). Neurobrucellosis in stranded dolphins, Costa Rica. *Emerg. Infect. Dis.* 14, 1430–1433. doi: 10.3201/eid1409.071056

Houde, M., Pacepavicius, G., Wells, R. S., Fair, P. A., Letcher, R. J., Alaee, M., et al. (2006). Polychlorinated biphenyls (PCBs) and hydroxylated polychlorinated biphenyls (OH-PCBs) in plasma of bottlenose dolphins (*Tursiops truncatus*) from the Western Atlantic and the Gulf of Mexico. *Environ. Sci. Technol.* 40, 5860–5866. doi: 10.1021/es060629n

Jackowski, C., Warntjes, M. J. B., Berge, J., Bär, W., and Persson, A. (2010). Magnetic resonance imaging goes postmortem: noninvasive detection and assessment of myocardial infarction by postmortem MRI. *Eur. Radiol.* 21, 70–78. doi: 10.1007/s00330-010-1884-6

Jefferson, T. A., Curry, B. E., and Kinoshita, R. (2002). Mortality and morbidity of Hong Kong finless porpoises, with emphasis on the role of environmental contaminants. *Raffles Bull. Zool.* 10, 161–171.

Klein, W. M., Kunz, T., Hermans, K., Bayat, A. R., and Koopmanschap, D. H. J. M. (2016). The common pattern of postmortem changes on whole body CT scans. *J. Forensic Radiol. Imaging* 4, 47–52. doi: 10.1016/j.jofri.2015.11.006

Kot, B. C. W., Fernando, N., Gendron, S., Heng, H. G., and Martelli, P. (2016). "The virtopsy approach: bridging necroscopic and radiological data for death investigation of stranded cetaceans in the Hong Kong waters," in *IAAAM 47th Annual Conference Proceedings*, (Virginia Beach, VA: IAAAM).

Kot, B. C. W., Chan, D. K. P., Yuen, A. H. L., and Tsui, H. C. L. (2018). Diagnosis of atlanto-occipital dissociation: standardised measurements of normal craniocervical relationship in finless porpoises (genus *Neophocaena*) using postmortem computed tomography. *Sci. Rep.* 8:8474. doi: 10.1038/s41598-018-26866-8

Kot, B. C. W., Chan, D. K. P., Yuen, A. H. L., Wong, F. H. M., and Tsui, H. C. L. (2019). Morphological analysis of the foramen magnum in finless porpoise (genus *Neophocaena*) using postmortem computed tomography 3D volume rendered images. *Mar. Mam. Sci.* 35, 261–270. doi: 10.1111/mms.12512

Kot, B. C. W., Chan, D. K. P., Chung, T. Y. T., and Tsui, H. C. L. (2020). Image rendering techniques in postmortem computed tomography: evaluation of biological health and profile in stranded cetaceans. *JoVE* (in press).

Levy, A. D., Harcke, H. T., and Mallak, C. T. (2010). Postmortem imaging: MDCT features of postmortem change and decomposition. *Am. J. Forensic Med. Pathol.* 31, 12–17. doi: 10.1097/paf.0b013e3181c65e1a

Lundström, C., Persson, A., Ross, S., Ljung, P., Lindholm, S., Gyllensvärd, F., et al. (2012). State-of-the-art of visualization in post-mortem imaging. *APMIS* 120, 316–326. doi: 10.1111/j.1600-0463.2011.02857.x

Mckenna, M. F., Goldbogen, J. A., Leger, J., Hildebrand, J. A., and Cranford, T. W. (2007). Evaluation of postmortem changes in tissue structure in the bottlenose dolphin (*Tursiops truncatus*). *Anat. Rec.* 290, 1023–1032. doi: 10.1002/ar.20565

McKinney, M. A., De Guise, S., Martineau, D., Beland, P., Lebeuf, M., and Letcher, R. J. (2006). Organohalogen contaminants and metabolites in beluga whale (*Delphinapterus leucas*) liver from two Canadian populations. *Environ. Toxicol. Chem.* 25, 30–41.

Montie, E., Schneider, G., Ketten, D., Marino, L., Touhey, K., and Hahn, M. (2007). Neuroanatomy of the subadult and fetal brain of the Atlantic white-sided dolphin (*Lagenorhynchus acutus*) from *in situ* magnetic resonance images. *Anat. Rec. (Hoboken)* 290, 1459–1479. doi: 10.1002/ar.20612

Oelschläger, H., Ridgway, S., and Knauth, M. (2010). Cetacean brain evolution: dwarf sperm whale (*Kogia sima*) and common dolphin (*Delphinus delphis)* – an investigation with high-resolution 3D MRI. *Brain Behav. Evol.* 75, 33–62. doi: 10.1159/000293601

Pfefferbaum, A., Sullivan, E. V., Adalsteinsson, E., Garrick, T., and Harper, C. (2004). Postmortem MR imaging of formalin-fixed human brain. *Neuroimage* 21, 1585–1595. doi: 10.1016/j.neuroimage.2003.11.024

Raga, J., Banyard, A., Domingo, M., Corteyn, M., Van Bressem, M., Fernández, M., et al. (2008). Dolphin *Morbillivirus* epizootic resurgence, Mediterranean Sea. *Emerg. Infect. Dis.* 14, 471–473. doi: 10.3201/eid1403.071230

Scheurer, E., Lovblad, K. O., Kreis, R., Maier, S. E., Boesch, C., Dirnhofer, R., et al. (2011). Forensic application of postmortem diffusion-weighted and diffusion tensor MR imaging of the human brain in situ. *AJNR Am. J. Neuroradiol.* 32, 1518–1524. doi: 10.3174/ajnr.a2508

Smith, A. B., Lattin, G. E., Berran, P., and Harcke, H. T. (2012). Common and expected postmortem CT observations involving the brain: mimics of antemortem pathology. *AJNR Am. J. Neuroradiol.* 33, 1387–1391. doi: 10.3174/ajnr.a2966

Thali, M. J., Yen, K., Schweitzer, W., Vock, P., Boesch, C., Ozdoba, C., et al. (2003a). Virtopsy, a new imaging horizon in forensic pathology: virtual autopsy by postmortem multislice computed tomography (MSCT) and magnetic resonance imaging (MRI) – a feasibility study. *J. Forensic Sci.* 48, 386–403.

Thali, M. J., Yen, K., Schweitzer, W., Vock, P., Ozdoba, C., and Dirnhofer, R. (2003b). Into the decomposed body–forensic digital autopsy using multislice-computed tomography. *Forensic Sci. Int.* 134, 109–114. doi: 10.1016/s0379-0738(03)00137-3

Tsui, H. C. L., Kot, B. C. W., Chung, T. Y. T., and Chan, D. K. P. (2020). Virtopsy as a revolutionary tool for cetacean stranding programs: implementation and management. *Front. Mar. Sci.* (in press).

Yen, K., Weis, J., Kreis, R., Aghayev, E., Jackowski, C., Thali, M., et al. (2006). Line-scan diffusion tensor imaging of the posttraumatic brain stem:

changes with neuropathologic correlation. *AJNR Am. J. Neuroradiol.* 27, 70–73.

Yuen, A. H. L., Tsui, H. C. L., and Kot, B. C. W. (2017). Accuracy and reliability of cetacean cranial measurements using computed tomography three dimensional volume rendered images. *PLoS ONE* 12:e0174215. doi: 10.1371/journal.pone.0174215

Zech, W. D., Schwendener, N., Persson, A., Warntjes, M. J., and Jackowski, C. (2015). Postmortem MR quantification of the heart for characterization and differentiation of ischaemic myocardial lesions. *Eur. Radiol.* 25, 2067–2073. doi: 10.1007/s00330-014-3582-2

Conflict of Interest: The authors declare that the research was conducted in the absence of any commercial or financial relationships that could be construed as a potential conflict of interest.